

# Structure Functions, Form Factors, and Lattice QCD \*

Walter Wilcox<sup>a</sup> and B. Andersen-Pugh<sup>b</sup>

<sup>a</sup>Department of Physics,  
Baylor University, Waco, TX 76798, USA

<sup>b</sup>Department of Physics,  
Luther College, Decorah, IA 52101, USA

We present results towards the calculation of the pion electric form factor and structure function on a  $16^3 \times 24$  lattice using charge overlap. By sacrificing Fourier transform information in two directions, it is seen that the longitudinal four point function can be extracted with reasonable error bars at low momentum.

## 1. INTRODUCTION

The direct calculation of hadron structure functions by current overlap techniques is based on the simulation of the Euclidean hadronic matrix elements  $\langle h(\mathbf{0}) | T[J_\mu(\mathbf{r}, t) J_\nu(0)] | h(\mathbf{0}) \rangle$ , where  $J_\mu = q_u J_\mu^u + q_d J_\mu^d$  is the full electromagnetic current and  $J_\mu^{d,u}$  are the  $d$ ,  $u$  quark flavor current densities. Such calculations are likely to be quite costly, so it seems worthwhile to check the validity of this approach by less ambitious calculations utilizing the basic current overlap technique. The longitudinal piece (corresponding to  $\mu = \nu = 0$  above, where  $J_0 = i\rho$ ) of structure functions for mesonic systems provides such a test[1]. We expect for the pion that vector dominance should hold, resulting in a known elastic limit for both the  $\rho^u \rho^u$  (same flavor) and  $\rho^d \rho^u$  (different flavor) sectors. This calculation serves to test whether the lattice size is large enough in space and time, the size of statistical errors, and other important issues. Since we use the conserved lattice current, there are also many useful numerical identities which serve as checks on the calculation. In constructing these four point functions, we make multiple use of the sequential source technique[2] for quark propagators. Our work so far indicates that the full electromagnetic amplitude should be attainable for low momentum transfers; however, we see no indications of inelastic contributions in our results. In this brief report we will concen-

trate on issues relating to systematics and statistical errors.

## 2. THE CALCULATION

### 2.1. The Current Overlap Technique

The structure function can be obtained from[3]

$$Q_{\mu\nu}(\mathbf{q}^2, t) = \sum_{\mathbf{r}} e^{-i\mathbf{q}\cdot\mathbf{r}} P_{\mu\nu}(\mathbf{r}, t) \quad (1)$$

where,

$$P_{\mu\nu}(\mathbf{r}, t) = \sum_{\mathbf{x}} \langle \pi^+(\mathbf{0}) | T[J_\mu(\mathbf{r} + \mathbf{x}, t) J_\nu(\mathbf{x}, 0)] | \pi^+(\mathbf{0}) \rangle. \quad (2)$$

It is the quantity  $P_{\mu\nu}(\mathbf{r}, t)$  which is directly calculated in our simulations. We may study the form factor by using the relation [4]

$$Q_{00}(\mathbf{q}^2, t) \xrightarrow{t \gg 1} \frac{(E_q + m_\pi)^2}{4E_q m_\pi} F^2(\mathbf{q}^2) e^{-(E_q - m_\pi)t}. \quad (3)$$

For this calculation we utilized a  $16^3 \times 24$  lattice and  $\beta = 6.0$  in the quenched approximation. We have omitted disconnected quark graph amplitudes because of the difficulty of simulating the corresponding correlation functions. In constructing the  $P_{00}(\mathbf{r}, t)$  there are three distinct classes of connected diagrams which contribute; see Figure 1 where the effect of the currents is represented by an “X”. The different flavor piece (Figure 1(a)) is calculated by combining quark propagator lines from source and sink; this

\*Talk presented by B. Andersen-Pugh.

Figure 1. Three types of connected current overlap diagrams: (a) different flavor; (b) same flavor direct; (c) same flavor Z-graph.

involves two quark inversions per configuration. In addition, the same flavor amplitude contains both “direct” (Figure 1(b)) and “Z-graph” (Figure 1(c)) contributions because of the indistinguishability of the two currents. These are calculated separately and the results added together; three additional propagators are needed to do this.

## 2.2. Fourier Reinforcement

It is the  $\mathbf{x}$  sum in equation (2) which is difficult to perform when the currents involve the same flavor because of quark lines going from  $(\mathbf{r} + \mathbf{x}, t)$  to  $(\mathbf{x}, 0)$  ( $\mathbf{r}$  and  $\mathbf{x}$  both summed). However, the statistical error bars on  $Q_{00}^{uu}(\mathbf{q}^2, t)$  were reduced by means of the following strategy. We use a charge density sheet operator,

$$\tilde{\rho}(z, t) = \sum_{x,y} \rho(x, y, z, t), \quad (4)$$

Using this when  $\mathbf{q} = q\hat{z}$ ,  $Q_{00}^{uu}(\mathbf{q}^2, t)$  can be written (using translational independence) as

$$Q_{00}^{uu}(\mathbf{q}^2, t) = N_z \sum_z e^{-iqz} \cdot \langle \pi^+(\mathbf{0}) | T[\tilde{\rho}(z, t)\tilde{\rho}(0, 0)] | \pi^+(\mathbf{0}) \rangle, \quad (5)$$

where  $N_z$  is the number of lattice points in the  $z$  direction.

Figure 2. Effect of using the extended operator  $\tilde{\rho}(z, t)$  at  $\kappa = .154$  on  $Q_{00}^{uu}(\mathbf{q}^2, t)$ . Diamonds: Fourier Reinforced data; squares: nonreinforced data. The line here and in Figure 3 is the expected vector dominance elastic limit.

Figure 2 illustrates the effect of using this technique at  $q = \frac{\pi}{8}$  and  $\kappa = .154$  on 10 configurations. The Fourier Reinforced (“FR”) result used the  $\tilde{\rho}(z, t)$  operator, whereas the nonreinforced result fixes  $\mathbf{x}$  in (2) to a single location[5]. The two results in Figure 2 are consistent with one another, although the FR result is systematically higher. Both are consistent with a single exponential behavior (no inelastic part), even at small time separations between the currents,  $t$ , although there is a mysterious bump in the FR result. This could be a statistical fluctuation or an effect of getting too near the sink interpolation fields. It is seen that the uncertainties in  $Q_{00}^{uu}(\mathbf{q}^2, t)$  are significantly reduced in the FR amplitude.

Figure 3. Diamonds: full electromagnetic amplitude,  $Q_{00}(\mathbf{q}^2, t)$ , equation (6); squares: different flavor amplitude,  $Q_{00}^{du}(\mathbf{q}^2, t)$ .

### 3. PRELIMINARY RESULTS

Zero momentum smeared pion interpolation fields are used at source and sink which are located on the time edges of the lattice in order to maximize the time extent available for measurements. Extensive numerical tests were performed on the  $Q_{00}^{du}(\mathbf{q}^2, t)$  amplitude to make sure nonvacuum contaminations do not occur; no such effects were seen. This quantity was reconstructed so that the two nonlocal, conserved charge densities were centered in time between the time edges. When measuring  $Q_{00}^{uu}(\mathbf{q}^2, t)$ , we used an extended source (*FR* case) or a point charge source (non *FR*) on time steps 8 and 9. Thus, the maximum time separation between the two charge operators is 15 in the same flavor case but 22 in the different flavor case.

We find that the the same flavor spatial correlation function is significantly smaller than the different flavor one. It is dominated by the direct graph; the Z-graph contributes only at small time separations and serves to make the correlation function marginally wider. At small  $t$  we see a spatial anisotropy similar to [6].

Figure 3 shows the full pion amplitude

$$Q_{00}(\mathbf{q}^2, t) = \frac{4}{9}Q_{00}^{du}(\mathbf{q}^2, t) + \frac{5}{9}Q_{00}^{uu}(\mathbf{q}^2, t), \quad (6)$$

again at  $q = \frac{\pi}{8}$  for  $\kappa = 0.154$  compared with the different flavor piece  $Q_{00}^{du}(\mathbf{q}^2, t)$  (for which the sum in (2) is easy). Using *FR*, the error bars on the full amplitude come under control. Both results are apparently tending to the vector dominance elastic limit.

It is possible to measure both elastic and inelastic processes from our hadronic amplitudes. The various different flavor amplitudes are especially useful because of their small error bars. They contain the information to do a survey of the form factors of all groundstate nonsinglet mesons.

### 4. ACKNOWLEDGMENTS

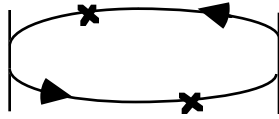
This work was partially supported by the National Center for Supercomputing Applications and the National Science Foundation under Grant PHY-9203306 and utilized the NCSA CRAY systems at the University of Illinois at Urbana-Champaign.

### REFERENCES

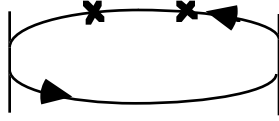
1. The longitudinal piece of the pion structure function vanishes at both low energies (no longitudinal photons) and high energies (Callan-Gross relation) and thus is almost purely elastic. This is in contrast to the transverse correlation function,  $Q_{ii}(\mathbf{q}^2, t)$  ( $i = 1, 2, 3$ ), which is purely inelastic.
2. See Refs. 12 in W. Wilcox, T. Draper and K.-F. Liu, Phys. Rev. **46D**, 1109 (1992).
3. W. Wilcox, in *Lattice 92*, Proceedings of the International Conference on Lattice Field Theory, Amsterdam, The Netherlands, 1992, edited by J. Smit and P. van Baal [Nucl. Phys. **B** (Proc. Suppl.)] **30** (1993) 491.
4. W. Wilcox, in *Lattice 91*, Proceedings of the International Symposium on Lattice Field Theory, Tsukuba, Japan, 1991, edited by M. Fukugita et. al. [Nucl. Phys. **B** (Proc. Suppl.)] **26** (1992) 406. Please note that equation (5) of this reference should read  $Q_{em}(q^2) >$

$F_\pi^2(q^2)$  and that the Figure 1 ordinate actually represents the extracted form factor,  $F_\pi(q^2)$ , rather than  $Q_{du}(q^2)$ .

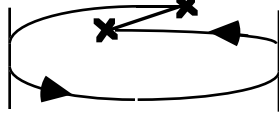
5. Fixing  $\mathbf{x}$  to a single location does not momentum smear the amplitude since we use zero momentum interpolation fields at the two ends.
6. M.-C. Chu, J. M. Grandy, S. Huang, and J. W. Negele, Phys. Rev. **48D**, 3340 (1993).



(a)



(b)



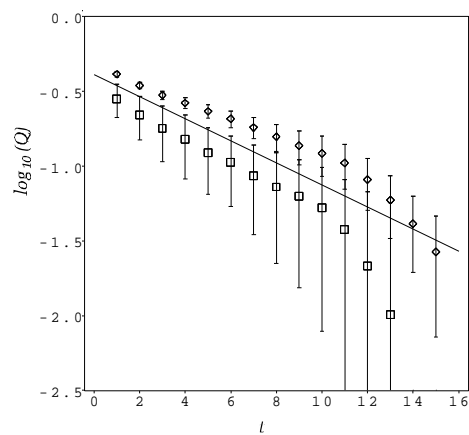
(c)

This figure "fig1-1.png" is available in "png" format from:

<http://arxiv.org/ps/hep-lat/9312034v1>

This figure "fig1-2.png" is available in "png" format from:

<http://arxiv.org/ps/hep-lat/9312034v1>



This figure "fig1-3.png" is available in "png" format from:

<http://arxiv.org/ps/hep-lat/9312034v1>

